Electromagnetic Acoustic Transducer for Detection and Characterization of Hidden Cracks inside Stainless Steel Material

H. Boughedda [1*], T. Hacib [1], Y. Le Bihan [2], M. Chelabi [1], and H. Acikgoz [3]

[1] L2EI Laboratory, Jijel University, BP 98 Ouled Aissa, Jijel 18000, Algeria
*houssem.boughedda@univ-jijel.dz

[2] Group of Electrical Engineering — Paris (GeePs)
CNRS - Univ. Paris-Saclay - CentraleSupelec - Sorbonne Univ, 11, rue Joliot Curie
91192 Gif sur Yvette Cedex, France

[3] Material Science Engineering Department, KTO Karatay University, Konya, Turkey

Abstract ─ Industrial structure are exposed to microstructural changes caused by fatigue cracking, corrosion and thermal aging. Generally, a hidden crack is very dangerous because it is difficult to detect by Non-Destructive Evaluation (NDE) techniques. This paper presents a new approach to estimate the hidden cracks dimensions inside a stainless steel plate based on the EMAT signal. The received signal by EMAT is simulated using the Finite Element Method (FEM). Then, the identification of the hidden crack sizes is performed via the combination of two techniques; the first one is the Time-of-Flight (ToF) technique which was applied to estimate the crack height by the evaluation of the difference between the ToF of the healthy form and the defective form. Then, the crack width is estimated by the solution of the inverse problem from the received signal based on a meta-heuristic algorithm called Teaching learning Based optimization (TLBO). The obtained results illustrate the sensitivity of the EMAT sensor to the variation of the crack sizes. Moreover, the quantitative evaluation of the cracks dimensions, show clearly the efficiency and reliability of the adopted approache.

Index Terms ─ Characterization of hidden cracks, FEM, NDE, Time-of-Flight, TLBO algorithm.

I. INTRODUCTION

The requirement of structural integrity has become an indispensable process to ensure the reliability of the system by detecting the apparition of damages. The development of non-destructive testing (NDT) techniques during the last century, provides an effective way to monitor the health of structures [1]. Electromagnetic Acoustic Transducer (EMAT) is an ultrasonic NDT technique that has offered a non-contact inspection of conductive materials, compared to traditional piezoelectric transducers [2]. One of the most important advantages of EMAT is its ability to generate several types of waves by simply changing its structure or excitation frequency, such as Rayleigh wave, longitudinal waves and shear waves. The advantage of the ultrasonic shear wave compared to other waves is its possibility to travel deep inside the materials with low energy loss, which makes it suitable for inspecting deep structures with high efficiency [3,4].

EMAT launches the magnetic forces into the conductive sample under test via three transduction mechanisms: Lorentz forces, magnetization forces and magnetostriction. However, the application of magnetizing and magnetostrictive forces is confined only in a ferromagnetic materials. Concerning the non-ferromagnetic materials, Lorentz forces have the major contribution to generate ultrasonic waves [5-7]. In this research, the transduction efficiency of a shear wave EMAT that is applied on stainless steel will be investigated, which means that only the Lorentz force transduction mechanism needs to be considered.

The examination of cracks using EMAT sensor has been widely investigated by a number of researchers. In [8], the first numerical model has been developed using the FEM, which was capable of modeling the transmitter and the receiver EMAT system. In [9], a new EMAT configuration has been proposed based on a periodic permanent-magnet (PPM) to generate and receive shear horizontal guided waves propagating in the circumferential direction. In [10], the estimation of the surface crack depth in pitch-catch mode by EMAT sensor has been proposed. It was carried out experimentally by determining the reflection and the transmission coefficients of Rayleigh waves scattered at a surface crack. However, this approach is limited only for the estimation of the cracks depth. In [11], the detection and localization of vertical cracks was

employed based on the diffraction phenomena of compressional waves by measuring the Time of Flight (ToF) of the diffracted waves. However, this approach has shown a low efficiency for assessing the crack width. In [12], a new approach for estimating the dimensions of surface cracks has been proposed. this approach is based on the combination of EMAT probe and partial least squares regression (PLSR) algorithm. This approach shows acceptable measurement accuracy in the sizing of the surface crack.

In recent years, the majority of EMAT researches have focused on cracks detection and to solve the problem of low conversion efficiency [13-15]. Whilst, the quantitative description of the defects didn't receive much concern. The main contribution of the current work is the detection and the characterization of hidden cracks inside a stainless steel plate. The cracks' height has been estimated using ToF technique in pulse-echo mode by measuring the time of flight of the transmitted and the reflected shear waves. This technique is based on the difference between the ToF of the healthy and the defective state of the inspected materials. Whereas, the cracks width has been estimated using a new stochastic optimization algorithm, that is called Teaching-Learning Based Optimization (TLBO) algorithm, which is used to solve the inverse problem from the EMAT signal. This technique was applied due to the linearity relation between the change in crack width and the received signal by EMAT. Moreover, TLBO algorithm has proved its efficiency over other stochastic algorithms [16,17].

The remainder of this paper is arranged as follows: first, developing a two dimensional (2D) numerical model of EMAT based on the FEM. This model includes an evaluation of the mechanical displacement and the output signal by EMAT. Then, the sensitivity of EMAT sensor to different hidden crack sizes has been checked. Finally, the identification of the cracks depth using ToF technique, and the characterization of the cracks width by combining TLBO algorithm and EMAT received signal.

II. EMAT SHEAR WAVE CONFIGURATION

Electromagnetic Acoustic Transducer (EMAT) configurations vary according to the type of waves that we want to produce during the test [9]. Usually, EMAT configurations consists of two main components, a magnet and a coil, which are placed above the material under test. EMAT probe can be used as a pulse-echo mode or on pitch-catch mode. In this work, the pulse-echo mode has been preferred to check the bottom of the stainless steel plate, i.e., the same transducer is used to generate and receive the shear and the longitudinal waves. The EMAT structure that is used in this work is shown in Fig. 1. It consists of a two adjacent permanent magnets above a spiral coil; each magnet produces

biasing field normal to the surface but in opposite direction (with flux density of 1 T). The coil and the permanent magnet have the same central axis. The test specimen is a non-magnetic material ($\mu=\mu_0$) represented as a stainless steel plate with electrical conductivity $\sigma=3.6\times10^6$ [S/m]. The spiral coil is made by copper with six turns, it is fed by an alternative current $i(t)$ with frequency $f=2$ MHz in order to create a dynamic magnetic field.
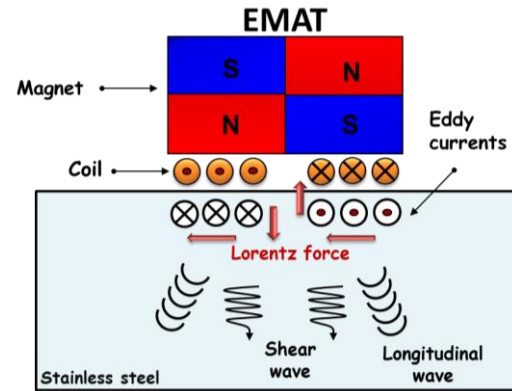

Fig. 1. Schematic representation the configuration and working principle of EMAT.

The eddy currents will be inducing at the surface of this the material due to this dynamic magnetic field [11]. The EMAT transduction mechanism in non-ferromagnetic material is the Lorentz force, which is generated by the interaction between the static magnetic field (from the permanent magnet) and the induced eddy currents. The Lorentz force launches elastodynamic waves (mechanical vibrations), which propagate inside the material under test [18]. In the receiving mode, the static magnetic field, of the receiver EMAT, interacts with the velocity of the mechanical displacement at the surface of the plate to generate spatial eddy currents underneath. These currents induce a voltage in the coil of the EMAT [12]:

$$i(t) = \beta\, e^{-\alpha.(t-\tau)^2} .\cos\left(2\pi f(t-\tau)\right), \qquad (1)$$

where, β is the current amplitude 5 (A), α is the bandwidth factor 4×10^{-12} (s^{-2}), τ is the arrival time $1(\mu s)$.

III. FINITE ELEMENT SIMULATION

A two-dimensional (2D) finite element simulation has been performed using the COMSOL Multiphysics software, to simulate the generation and the reception of the ultrasonic waves by EMAT, based on the combination of electromagnetic and mechanical models. The simulation includes an evaluation of the eddy current, the magnetic flux density, the Lorentz force, the mechanical displacement inside the stainless steel plate and the output voltage by the EMAT.

A. Governing equations

The Maxwell's equations are used to calculate the static magnetic field and the distribution of induced eddy currents in the aluminum plate [4]. After some manipulations, we get the following Partial Deferential Equation (PDE):

$$\nabla \times (\frac{1}{\mu}(\nabla \times A_z - B_r)) + \sigma\frac{\partial A_z}{\partial t} - \sigma v \times (\nabla \times A_z) + \sigma\nabla V = J_{ex} , \quad (2)$$

where σ, μ, v, J_{ex} and B_r are conductivity, permeability, velocity, external current density of the coil and magnetic flux density respectively.

The solving of (2) in static and transient analysis allows calculating the MVP A_z, which used to calculate the static magnetic field B_s and the induced current J_e in the conductive material:

$$B_s = \nabla \times A_z , \quad (3)$$

$$Je = -\sigma\frac{\partial A_z}{\partial t} . \quad (4)$$

By considering that the Lorentz force as the only contribution body force and the material as satisfying the continuous elastic isotropic, we have Navier's equation [18]:

$$-\mu\nabla \times \nabla \times \mathbf{u} - (\lambda + \mu)\nabla(\nabla.\mathbf{u}) + \rho\frac{\partial^2\mathbf{u}}{\partial t} = \mathbf{F}_L . \quad (5)$$

where λ and μ are the Lame constants.

The ultrasonic wave produced in the stainless steel plate, with length of 200 mm and thickness of 20 mm. The plate has the following properties: Young's modulus of 210 GPa, Poisson's ratio of 0.28, mass density of 7850 kg/m^3.

B. Lorentz force evaluation

The Lorentz force $\mathbf{F}_L$ results by the interaction of the current density J_e and the static magnetic flux density B_S that were calculated in transient and static analysis respectively, according to the following equation [18]:

$$\mathbf{F}_L = J_e \times B_s . \quad (6)$$

Figure 2 shows the eddy currents density at the surface of the plate, which is extracted under wires 1 and 6. It can be observed that the eddy currents under wires 1 and 6, have the same density but in opposite directions; this is due to the excitation current in the EMAT coils.

Figures 3 and 4 show the spatial distribution and the density of the Lorentz force in the x-direction $\mathbf{F}_L(x)$ at the surface of the plate. It appears that the $\mathbf{F}_L(x)$ density has the same density and direction under each coil segment; this is due to the non-uniformity of the B_y under the two symmetrical sides of the coil.

C. Shear wave generation

Figure 5 shows the time history of the mechanical displacement that has been extracted at the bottom of the plate (see Fig. 6 (b)). The first upcoming wave is the longitudinal wave at the moment 34 μs and the second

reaching wave is the shear wave at the moment 63 μs. This time is called the Time of Flight (ToF) of the waves [16]. The longitudinal and shear wave velocity in the stainless steel material are C_l=5.8 mm/μs and C_s=3.2 mm/μs respectively [9].
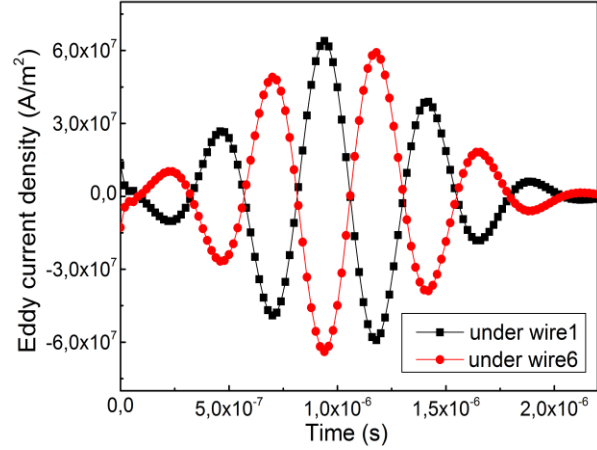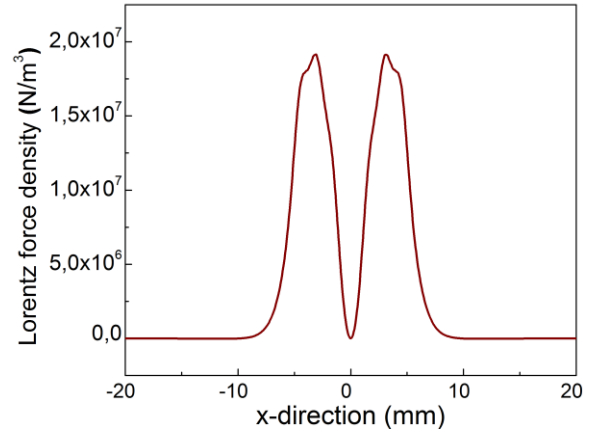

Fig. 2. Eddy current density under wire 1 and 6.
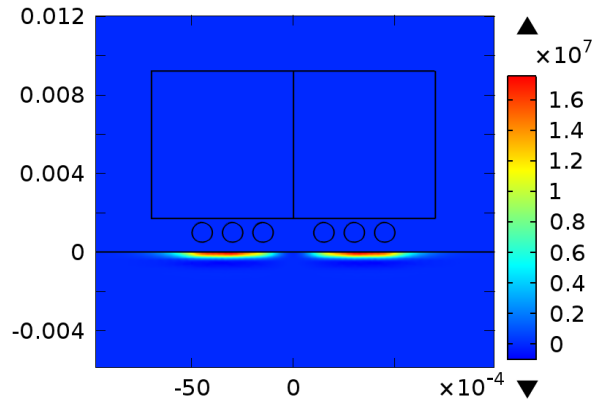

Fig. 3. Lorentz force density $F_L(x)$ at the surface edge.

Fig. 4. Spatial distribution of the Lorentz force $F_L(x)$.

Table 1 summarizes the comparison results between the theoretical velocity and the simulation velocity for the longitudinal and shear waves diffused in the material. From the observed error (0.81% ~ 1.41%), it can be said that there is a good agreement between theoretical and simulation velocity waves, which mean the reliability of the EMAT model to identify the hidden cracks dimensions.
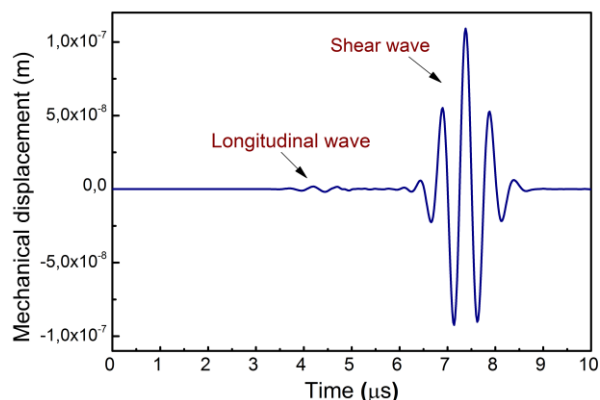

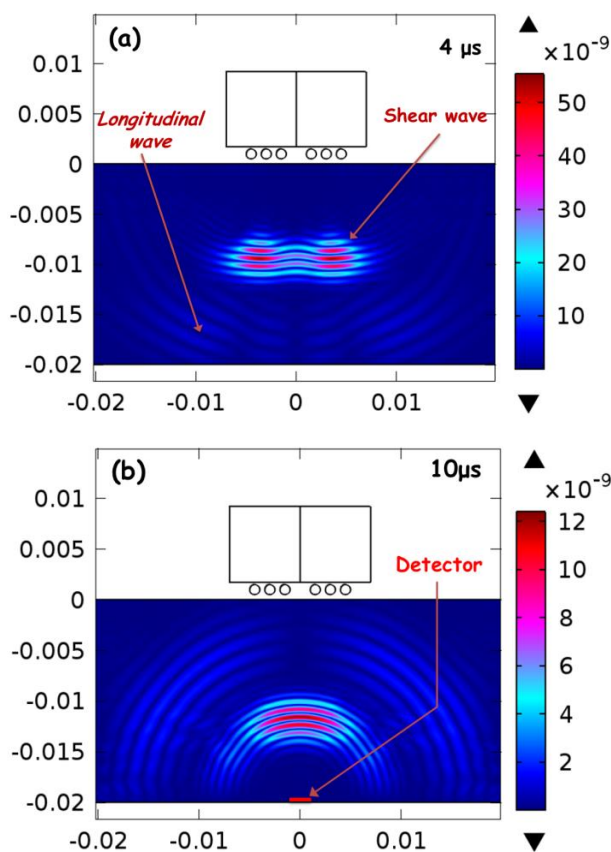Fig. 5. Mechanical displacement at the bottom of plate.

Fig. 6. Mechanical field distribution: (a) transmitted mode at (4.5 µs), and (b) reflected mode at (10.5 µs).

Table 1: Validation of the ultrasonic waves velocity

Wave Mode	Theoretical Velocity	Simulation Velocity	MAPE (%)
Shear wave	3200 (m/s)	3174 (m/s)	0.81%
Longitudinal	5800 (m/s)	5882 (m/s)	1.41%

The ultrasonic waves generated by EMAT are illustrated in Fig. 6 (a); at the instant 4 µs after the EMAT excitation, we can distinguish two types of waves. The first wave generated is the longitudinal wave, that seems faster but with low diffusion strength. The second is the shear wave; it diffuses straight towards the bottom of the plate. Moreover, it appears stronger compared to the longitudinal wave. Figure 6 (b) shows the reflected ultrasonic waves at instant 10 µs.

IV. CHARACTERIZATION OF THE HIDDEN CRACKS

A. Characterisation of cracks height by ToF

Time-of-Flight approach is a technique employed to measure the distance between the sensor and the targets for each point during the scan, see Fig. 7. The EMAT probe sends out an ultrasonic signal (pulse), and then picks up the returning information (echoes) from the bottom edge to the EMAT probe, i.e., measuring the round trip time of the EMAT signal.
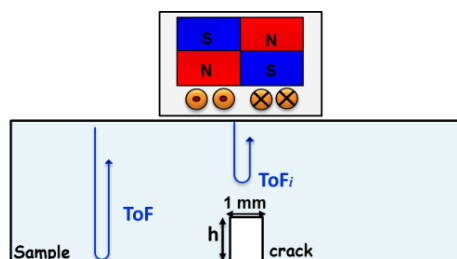

Fig. 7. Schematic represents the methodology cracks height evaluation using ToF technique.
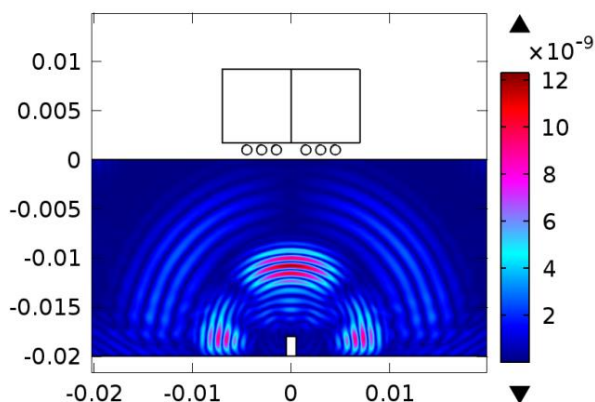

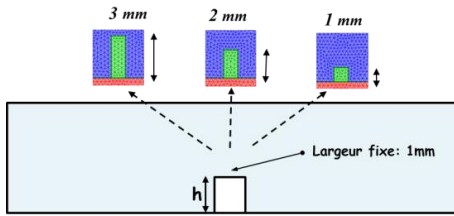Fig. 8. Reflected ultrasonic waves from the hidden crack.
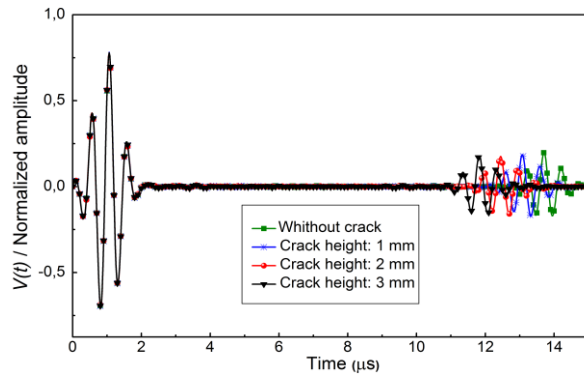
Fig. 9. Schematic represents the cracks dimensions
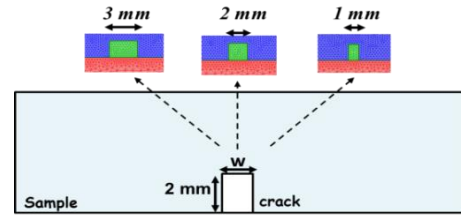

Fig. 11. Schematic represents the cracks dimensions.

Fig. 10. Mechanical displacement for different hidden cracks height.

Fig. 12. Mechanical displacement for different hidden cracks width.

The crack height is calculated via multiplying the shear wave velocity C_s and the difference between the ToF of the healthy shape and that of the defective shape (ToF$_i$) according to the following expression:

$$h_i = \left[C_s \times \left(ToF - ToF_i \right) \right] / 2 . \qquad (7)$$

In this section we introduce an artificial crack at the bottom of the stainless steel plate. Figure 8 shows the interaction of the ultrasonic waves with the hidden crack. The model was checked for five different sizes of cracks height as shown in Fig. 9.

The amplitude of the output signal $V(t)$ by EMAT was recorded for the different sizes that are proposed. The results shown in Fig. 10, prove that the model is able to detect the existence and the changes in the crack height; this is due to the reflection caused by the presence of the hidden cracks. Table 2 presents a comparison between the desired cracks height and the estimated crack height by ToF technique. The observed Error show clearly the efficiency of the ToF approach to estimate hidden crack height.

Table 2: Estimated and desired crack height by ToF

Crack No:	ToF(i) μs	Crack Height (m)		MAPE (%)
		Estimated	Desired	
1	11.9	0.96×10^{-3}	1×10^{-3}	4%
2	11.28	1.95×10^{-3}	2×10^{-3}	2.4%
3	10.9	2.57×10^{-3}	2.5×10^{-3}	2.8%
4	10.56	3.1×10^{-3}	3×10^{-3}	3.3%
5	10.2	3.6×10^{-3}	3.5×10^{-3}	2.9%

B. Characterisation of cracks width by TLBO

The sensitivity of EMAT to the variation of the cracks width has been checked; the crack height is fixed at 2 mm while the width is varied from 1 to 3 mm, see Fig. 11. The output signal is illustrated in Fig.12; the efficiency of the EMAT sensor to detect the crack width variation is clearly shown. Moreover, the results prove that the change of crack width involves a change in the received signal. In the next, we propose a hidden crack with unknown width, and measure the received signal by EMAT sensor. The crack width has been estimated by resolved an inverse problem. Inverse problems in NDT field are mostly stated in order to solve the optimization problems. The numerical model such as FEM is used to represent the forward problem. However, iterative methods are used to solve the inverse problem in order to deduce geometrical information about the defects [12].

In this section, the Teaching Learning Based Optimization (TLBO) algorithm is used to estimate the hidden crack width via the resolve of the inverse problem from the acquired EMAT signal. The TLBO algorithm was proposed by *Rao*; the main idea in TLBO algorithm is the philosophy of teaching and learning approach. TLBO is a meta-heuristic method for global optimization; it is easy to implement, it can be applied to unconstrained or constrained problems. *Rao and Waghmare* have been applied for many multi-objective unconstrained and constrained test functions; the results were compared with other optimization algorithms and have demonstrated

that TLBO technique is faster and precise [19]

The algorithm of this method depends on a random initialization of the population in the feasible region. The process of TLBO is divided into two phases namely: the 'Teacher Phase' and the 'Learner Phase'. In teacher phase, the teacher is considered as a highly knowledgeable person in the class and imparts his knowledge directly to learners; the best solution is considered as the teacher. Supposed that a good teacher is the one who improves his/her learners up to his/her level in terms of knowledge. In learner phase, the interaction of learners one with another is the basic idea of this phase, so random interaction between learners improves their knowledge. Several investigations have improved the performance of the TLBO algorithm and have proved that this algorithm is a powerful and a very useful tool for the optimization problems; TLBO code-algorithm and more details are available in [17]. The code of TLBO is written in MATLAB software.

The inverse problem is an evaluation of cracks width by minimizing a predefined objective function. That was formulated by the Root Mean Square Error (RMSE), which represents the differences between predicted signal $V(x_i)$ and desired output signal V_d, the objective function can be written as follows:

$$\begin{cases} minimize\ f(X),\ X = (x_i) \\ f(X) = RMSE = \sqrt{\dfrac{1}{N}\sum_{i=1}^{N}(V_d - V(x_i))^2} \end{cases}, \quad (8)$$

where x_i represent the cracks width, the hidden crack width ranges from 250μm to 3 mm, which are distributed randomly in the investigation space N.
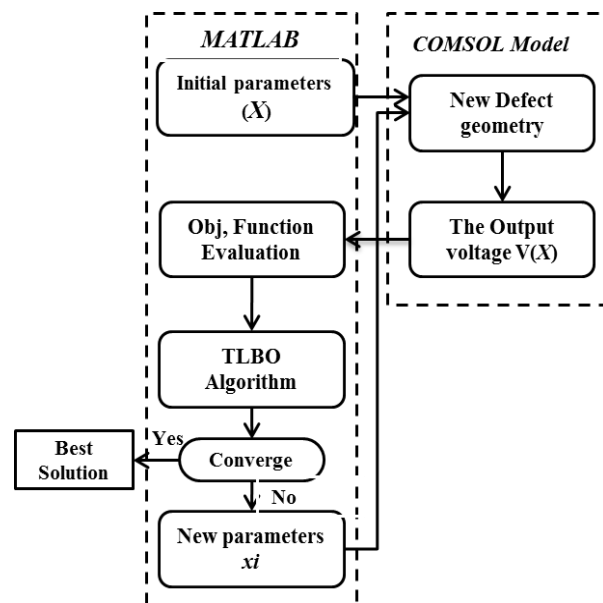

Fig. 13. Flowchart of the estimation process of the crack width by TLBO algorithm.

The resolution of the inverse problem has been carried out by the resolution of the forward problem that represented an evaluation of the output voltage in COMSOL Multiphysics. Then, the TLBO algorithm has been performed in MATLAB. Accordingly, the exhibited steps in Fig. 13 should be followed.

- Firstly, the initial parameter x_i are chosen randomly by TLBO algorithm.
- Secondly, the corresponding signal $V(X)$ of each parameter x_i is evaluated in COMSOL software. Then, the values of $V(X)$ is loaded in MATLAB in order to formulate the objective function that was represented in (8).
- Next, the TLBO algorithm is used to solve the inverse problem. The objective function has been evaluated several times for each iteration.
- Finally, if the stopping criteria is verified, the algorithm stops, otherwise, the algorithms choses new parameters from the investigation space, and repeat the evaluation of the algorithm loop until the stop criteria is verified.

Table 3: The estimated and desired width by TLBO

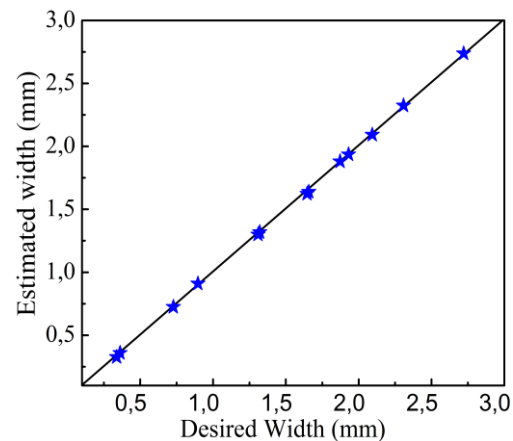| Defect No:	Cracks Width (m)		MAPE %
	Estimated	Desired	
1	$0{,}95 \times 10^{-3}$	1×10^{-3}	5%
2	$1{,}55 \times 10^{-3}$	$1{,}5 \times 10^{-3}$	3.3%
3	$2{,}08 \times 10^{-3}$	2×10^{-3}	4%
4	$2{,}45 \times 10^{-3}$	$2{,}5 \times 10^{-3}$	2%
5	$2{,}92 \times 10^{-3}$	3×10^{-3}	2.7%

Fig. 14. Comparison of Desired and estimated of crack width by TLBO algorithm.

Table 3 shows five values of crack width desired and its corresponding estimated width using TLBO algorithm. According to the obtained results in Fig.14, it can be said that the estimation cracks width by TLBO has given results very close to the expected values, and the MAPE observed show clearly the effectiveness of

the adopted algorithm to deduce the crack width.

VI. CONCLUSION

In this work, the EMAT probe is used to generate vertical shear waves inside a stainless steel plate for the detection and characterization of the hidden cracks. ToF technique is applied to evaluate the cracks height via the comparison of the ToF between the healthy shape and the defective shape. Then, the cracks width is estimated by resolving the inverse problem from the acquired EMAT signal based on TLBO algorithm. The FEM method that was implemented in the software COMSOL Multiphysics is employed to model the generation and the reception of the ultrasonic waves by EMAT, which involved the resolve of the electromagnetic and the mechanical fields. According to the achieved results, the EMAT model illustrates a high sensitivity to the existence or the change in the size of the hidden cracks. Moreover, the results have clearly shown the efficiency and the accuracy of the adopted approach to deduce the hidden cracks dimensions.

REFERENCES

[1] P. Burrascano, S. Callegari, A. Montisci, M. Ricci, and M. Versaci, "Ultrasonic nondestructive evaluation systems: Industrial application issues," *Springer*, pp. 1-4, 2015.

[2] B. Helifa, M. Féliachi, I. Lefkaier, F. Boubenider, A. Zaoui, and N. Lagraa, "Characterization of surface cracks using Eddy current NDT simulation by 3D-FEM and inversion by neural network," *Applied Computational Electromagnetics Society Journal*, vol. 31, no. 2, pp. 187-194, 2016.

[3] J. Parra-Raad, P. Khalili, and F. Cegla, "Shear waves with orthogonal polarisations for thickness measurement and crack detection using EMATs," *NDT & E. Int.*, vol. 111, p. 102212, 2020.

[4] M. Chelabi, T. Hacib, Y. Le Bihan, N. Ikhlef, H. Boughedda, and M. Mekideche, "Eddy current characterization of small cracks using least square support vector machine," *J. Phys. D: Appl. Phys.*, vol. 49, no. 15, 155303, 2016.

[5] R. Ribichini, F. Cegla, P. Nagy and P. Cawley, "Study and comparison of different EMAT configurations for SH wave inspection," *IEEE Trans Ultrason Ferroelectr Freq Control*, vol. 58, no. 12, pp. 2571-2581, 2011.

[6] K. Mirkhani, C. Chris, M. Chris, J. Maciej, D. Tomas, S. Anthony, J. R. Shapoorabadi, K. Adalbert, and P. Marcello, "Optimal design of EMAT transmitters," *NDT & E. International*, vol. 37, no. 3, pp. 181-193, 2004.

[7] R. Dhayalan, A. Kumar, B. Rao, and T. Jayakumar, "A hybrid finite element model for spiral coil electromagnetic acoustic transducer (EMAT)," *Int. J. Appl. Electromagn. Mech.*, vol. 46, no. 3, pp. 491-500, 2014.

[8] R. Ludwig, Z. You, and R. Palanisamy, "Numerical simulations of an electromagnetic acoustic transducer-receiver system for NDT applications," *IEEE Trans. Magn.*, vol. 29, no. 3, pp. 2081-2089, 1993.

[9] M. Hirao and H. Ogi, "An SH-wave EMAT technique for gas pipeline inspection," *NDT & E. Int.*, vol. 32, no. 3, pp. 127-132, 1999.

[10] C. He, D. Peng, L. Yan, L. Xiucheng, L. Zenghua, J. Jingpin, and W. Bin, "Estimation of surface crack depth using Rayleigh waves by electro-magnetic acoustic transducers," *Int. J. Acoust. Vibr.*, vol. 22, no. 4, 2017.

[11] N. Yacef, T. Bouden, and M. Grimes, "Accurate ultrasonic measurement technique for crack sizing using envelope detection and differential evolution," *NDT & E. International*, vol. 102, pp. 161-168, 2019.

[12] H. Boughedda, T. Hacib, Y. L. Bihan, and H. Acikgoz, "Cracks characterization of non-ferro-magnetic material using emat probe and PLSR technique," *PIER C. J.*, vol. 103, pp. 199-209, 2020.

[13] C. Pei, S. Zhao, P. Xiao, and Z. Chen, "A modified meander-line-coil EMAT design for signal amplitude enhancement," *Sens. Actuators, A*, vol. 247, pp. 539-546, 2016.

[14] Z. Cai, Y. Yan, and G. Tian, "Enhancement of Lamb-EMAT signal using a modified one-side pitch-catch design," *IEEE Access*, vol. 7, pp. 138556-138566, 2019.

[15] C. Thring, S. Hill, S. Dixon, and R. Edwards, "The effect of EMAT coil geometry on the Rayleigh wave frequency behaviour," *Ultrasonics*, vol. 99, p. 105945, 2019.

[16] A. Habibpour-Ledari and F. Honarvar, "Three dimensional characterization of defects by ultra-sonic time-of-flight diffraction (ToFD) technique," *J. Nondestr. Eval.*, vol. 37, no. 1, 2018.

[17] H. R. E. H Bouchekara and M. Nahas, "Optimization of electromagnetics problems using an improved teaching-learning-based-optimization technique," *Applied Computational Electromag-netics Society Journal*, vol. 30, no. 12, pp. 1341-1347, 2015.

[18] S. Wang, R. Su, X. Chen, L. Kang, and G. Zhai, "Numerical and experimental analysis of unidirectional meander-line coil electromagnetic acoustic transducers," *IEEE Trans. Ultrason. Ferroelectr. Freq. Control*, vol. 60, no. 12, pp. 2657-2664, 2013.

[19] R. Rao, V. Savsani, and D. Vakharia, "Teaching–learning-based optimization: A novel method for constrained mechanical design optimization problems," *Computer-Aided Design*, vol. 43, no. 3, pp. 303-315, 2011.